

This is the postprint (accepted) version of the final paper, published afterwards, here: <https://doi.org/10.1016/j.ejmech.2018.12.003>

We thank Elsevier for the opportunity.

Polycyclic maleimide-based derivatives as first dual modulators of neuronal calcium channels and GSK-3b for Alzheimer's disease treatment

Alessandra Bisi*, Raquel L. Arribas, Matteo Micucci, Roberta Budriesi, Alessandra Feoli, Sabrina Castellano, Federica Belluti, Silvia Gobbi, Cristobal de los Rios, Angela Rampa*

Abstract: Current healthcare has significantly increased the average life expectancy, leading to a consequently greater incidence of age-related diseases, such as Alzheimer's disease. Following a multitarget approach, in this paper a series of polycyclic maleimide-based derivatives were designed and synthesized aimed at simultaneously modulate neuronal calcium channels and glycogen synthase kinase 3-beta (GSK-3b), validated targets to combat Alzheimer' disease. Different structural modifications were performed on the polycyclic scaffold in order to investigate the structure-activity relationships and compound 10 emerged as a promising non-toxic lead compound, endowed with calcium modulating brain-addressed properties and significant GSK-3b inhibitory activity. Moreover, the easily affordable polycyclic core appears as a new appealing privileged structure in medicinal chemistry.

Keywords: Alzheimer's disease, Maleimide-based polycyclic scaffold, Ca²⁺ channels, GSK-3b, Dual inhibitors

1. Introduction

Alzheimer's disease (AD), the leading cause of dementia, is a multifactorial pathology resulting from a complex network of interrelated and not fully deciphered factors, and a long-term effective therapy remains at the top of the list for unmet needs [1]. A promising advanced drug discovery approach to treat disorders with such intricate pathological mechanisms consists in designing multi-target-directed ligands (MTDLs), able to simultaneously interfere with different biochemical and physiological processes that often concurrently occur [2].

In this scenario, multiple lines of evidence have implicated calcium dysregulation in brain aging and dementia [3]. Calcium ions are critical mediators of cell signaling both for their electrogenic functions (calcium-induced changes in membrane potential) and for their roles as intracellular messengers (activation of calcium-dependent enzymes). Accordingly, processes that result in compromised calcium signaling can lead to a range of pathophysiological conditions, such as hypertension, cardiac hypertrophy and a vast array of neurological problems [4]. Cellular calcium influx is mediated by specific channels, membrane-spanning proteins among which voltage-gated calcium channels (VGCCs) play a pivotal role in regulating calcium current in response to membrane depolarization. Their activity is essential to couple electrical signals in the cell surface to physiological events in cells. The family of VGCCs consists of ten members, which have been characterized in mammals, and serve distinct roles in cellular signal transduction. According to the nomenclature adopted in 2000, the CaV1 sub-family (Ca 1.1 to Ca 1.4) comprises L-type Ca²⁺ channels (LTCCs), VV responsible for long-lasting (L)-type Ca²⁺ currents and activated after strong depolarization [5]. LTCCs play a key role in the regulation of vascular smooth muscle contraction, and substances that interfere with their function (Ca²⁺ channel blockers, whose prototypes include 1,4-dihydropyridines, DHPs) are widely used in the therapy of hypertension.

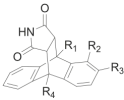
Considering the central role of Ca^{2+} in brain signaling functions, its imbalance is likely to be one of the main triggering causes of neurodegeneration. Moreover, b-amyloid peptide (Ab), responsible for the formation of senile plaques, one of the main AD hallmarks, can induce neuronal membrane-associated oxidative stress, resulting in disruption of intracellular calcium homeostasis and making neurons vulnerable to calcium overload [6]. Accordingly, the neuronal death elicited by the imbalance of this ion, observed during disease evolution, suggests that drugs restoring the proper Ca^{2+} levels in neurons might be a viable therapeutic option for AD [7]. Furthermore, Ca^{2+} channel blockade reduces Ab-induced neuronal decline in vitro, leading to neuroprotective effects in animal models [8].

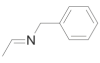
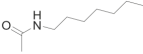
Some years ago, we reported a series of new anthracene- maleimide-based LTCC blockers, among which **1** (Fig. 1) emerged as the most promising compound [9]. Functional studies showed that **1** (lacking intracellular effects in vascular smooth muscle) would preferentially bind to inactivated LTCCs, directly interacting with the pore-forming subunit of the channel, suggesting a competitive interaction with the DHPs binding domain [9].

The maleimide-based polycyclic scaffold of compound **1** is recognized as a valuable template in different fields of medicinal chemistry, when decorated with appropriate substituents [9,10]. Focusing on therapeutic targets for AD, literature reports on inhibitors of glycogen synthase kinase-3b (GSK-3b) bearing the maleimide moiety [11e14]. Indeed, GSK-3b plays a pivotal role in the brain, where it regulates many crucial cellular processes, and its dysregulation proved to be involved in the development of many diseases, including AD. In this context, GSK-3b is the main kinase responsible for tau phosphorylation, and intracellular aggregates of hyperphosphorylated tau lead to the formation of neurofibrillary tangles, another major hallmark for AD [15]. Thus, it is increasingly evident that the role of hyperphosphorylation of tau in destabilization of microtubule assembly and disturbance of axonal transport is detrimental in the neurodegenerative process, whereby GSK-3b is widely considered a therapeutic target of interest, both in pharmaceutical and academic laboratories [16].

Pursuing our efforts toward the development of small-molecules as putative drug candidates for the treatment of AD, we turned our attention to calcium channels as a new therapeutic target to be exploited. Taking advantage of our previously reported LTCC blockers, here we report a new series of maleimide- anthracene-based compounds **2e10** (Fig. 1 and Table 1), in which different chemical modifications on the polycyclic scaffold were performed to deeply define structure activity relationship (SAR) studies against LTCCs. In particular, the effect elicited by various electron-withdrawing and electron-donating groups in different positions of the scaffold was investigated. Moreover, in a multi-target perspective and considering the presence of the maleimide moiety in different GSK-3b inhibitors, the new compounds were also evaluated for their activity on this key kinase.

Table 1



Compound	R ₁	R ₂	R ₃	R ₄
1	H	H	Cl	H
2	H	Cl	H	H
3	Cl	H	H	Cl
4	H	NH ₂	H	H
5	H	NHCOCH ₃	H	H
6	H	H	NH ₂	H
7	H	H	NHCOCH ₃	H
8	H	H	COCH ₃	H
9		H	H	H
10		H	H	H

2. Results

2.1 Chemistry

According to Scheme 1, compounds 2-6 and 8-10 were prepared via Diels-Alder cycloaddition, starting from maleimide and the appropriately substituted anthracenes 11-18. Compound 7 was obtained by acetylation of compound 6 with acetyl chloride in the presence of K_2CO_3 .

Not commercially available anthracenes 14, 17 and 18 were synthesized according to Scheme 2. 1-Aminoanthracene was acetylated with acetyl chloride in the presence of K_2CO_3 to obtain 14. The imine 17 resulted from the Schiff reaction of anthracene-9-carbaldehyde with benzylamine. The amide 18 was synthesized by condensation of the chloride of anthracene-9-carboxylic acid with heptan-1-amine.

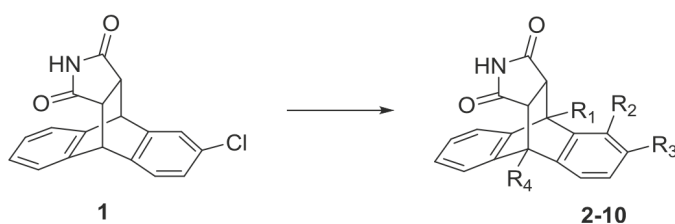


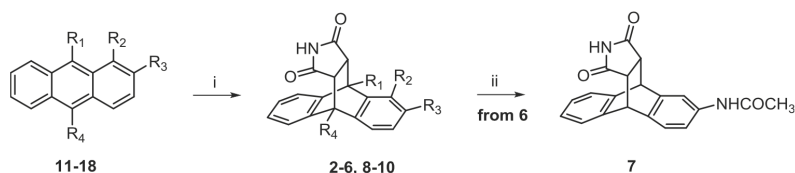
Fig. 1. Design of the new compounds.

2.2 Biological evaluation

2.2.1 Functional study on cardiac system

The new compounds (2-10, Table 1) were tested for their cardiovascular profile on isolated guinea pig left atrium driven at 1 Hz and on a spontaneously beating right atrium, to evaluate their inotropic and chronotropic effects, respectively. For compounds devoid of negative chronotropic activity, the inotropy was also checked in spontaneously beating right atria. Compound 1 and nifedipine were also tested as reference compounds. Indeed due to the peculiar structure of the compounds, this study was performed in order to exclude a possible relevant binding to cardiac calcium channels, which could be responsible for not negligible side effects.

From a first glance at the results (Table 2), all the tested molecules (1e10) showed interesting cardiovascular activity profile. Indeed, all derivatives displayed negative inotropic properties, with the exception of compound 8, bearing a strong electron-withdrawing group in R_3 . This effect was also observed on the right atrium in spontaneous activity, except for 5. In this respect, chlorine atoms gave the best results (compounds 1e3) and are better accommodated at C9-C10 positions, being 3 the most active derivative.

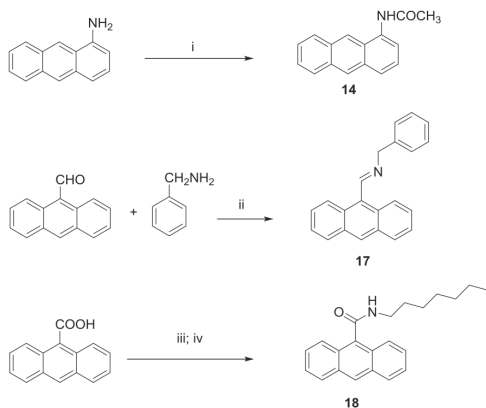


- 11, 2: $R_1 = \text{H}; R_2 = \text{Cl}; R_3 = \text{H}; R_4 = \text{H}$
 12, 3: $R_1 = \text{Cl}; R_2 = \text{H}; R_3 = \text{H}; R_4 = \text{Cl}$
 13, 4: $R_1 = \text{H}; R_2 = \text{NH}_2; R_3 = \text{H}; R_4 = \text{H}$
 14, 5: $R_1 = \text{H}; R_2 = \text{NHCOCH}_3; R_3 = \text{H}; R_4 = \text{H}$
 15, 6: $R_1 = \text{H}; R_2 = \text{H}; R_3 = \text{NH}_2; R_4 = \text{H}$
 16, 8: $R_1 = \text{H}; R_2 = \text{H}; R_3 = \text{COCH}_3; R_4 = \text{H}$
 17, 9: $R_1 = \text{CH=NCH}_2\text{C}_6\text{H}_5; R_2 = \text{H}; R_3 = \text{H}; R_4 = \text{H}$
 18, 10: $R_1 = \text{CONHC}_7\text{H}_{15}; R_2 = \text{H}; R_3 = \text{H}; R_4 = \text{H}$

Scheme 1. Preparation of compounds **2–10**. Reagents and conditions: i) Maleimide, toluene, reflux 5 h; ii) CH_3COCl , K_2CO_3 , acetone, reflux 3 h.

On the contrary, 1-10 were all devoid of chronotropic properties. Therefore, an appreciable selectivity of action can be noticed for the new derivatives, since nifedipine showed inotropic effects as well as negative chronotropic activity in the same experimental conditions. For sake of clarity, the results reported on Table 2 were also depicted in Fig. 2.

To assess the calcium antagonist activity of compounds 1-10, the inhibition of Ca^{2+} -induced contraction on K^+ -depolarized (80mM) guinea-pig vascular (aortic strips) and non-vascular (ileum) smooth muscle was evaluated. As reported in Table 3 and Fig. 3, opposite to nifedipine, the compounds did not display any vasorelaxant activity on aorta. On the contrary, all compounds, except derivative 5, showed a calcium antagonist action on non-vascular smooth muscle, with EC_{50} values ranging from 0.49 to 14.66 mM. This feature could be related to a selective modulation of calcium influx on non-vascular smooth muscle, making these derivatives devoid of relevant effects on blood pressure.



Scheme 2. Preparation of anthracene derivatives **14**, **17–18**. Reagents and conditions: i) CH_3COCl , K_2CO_3 , acetone, reflux 3 h; ii) toluene, reflux 24 h; iii) SOCl_2 , reflux 4 h; iv) heptan-1-amine, triethylamine, CH_2Cl_2 , r.t. 3 h.

2.2.2 Effect on Ca^{2+} entry through neuronal VGCC

To evaluate the blocking activity of the new derivatives, we stimulated SH-SY5Y neuroblastoma cells with an extracellular solution containing KCl 70 mM, leading to membrane depolarization and VGCC opening, what induced $[\text{Ca}^{2+}]$ elevation in the SH-SY5Y cells cytosol. The presence of compounds 1-3 and 10 at the concentration of 10 mM mitigated such elevation better than the well-known Ca^{2+} -antagonist nimodipine [18], used as standard in these experiments (Table 4, center column). The ability of these four active compounds to reduce the 70 mM K^+ -exerted neuronal Ca^{2+} increase was further assessed at different concentrations, with the aim of calculating, by sigmoidal regression, their inhibitory concentration 50 (IC_{50}), defined as the concentration of compound capable of halving the K^+ -elicited Ca^{2+} elevation (Table 4, right column). These compounds had IC_{50} s around 10 mM, being compound 10, with an IC_{50} of 9 mM, the best VGCC blocker.

Gathering all the results, some SAR can be extracted. The presence of chlorine atoms in 1-3 is well accepted to feature a proper blocking activity, unlike the presence of more polar groups, such as amines, imines or amides. Indeed, it is widely known that chlorine atoms are nicely accommodated in hydrophobic pockets. For this reason, the long-chain, highly hydrophobic substituents found in 10 provide positive outcomes, despite the presence of a polar group (amide) in an inner position. This hypothesis is confirmed by comparing the blocking effect of 7 with that of 8, where the replacement of the polar amide by the medium polar ketone increased the blocking activity from 8 to 20% (Table 4). Otherwise, the change of the substituted position in the aromatic rings did not play a key role in the blocking activity of the compounds. Overall, these results underline that non-polar substitution on these poly- cyclic derivatives enhances their VGCC blocking activity.

Table 2
Activity of tested compounds on cardiac parameters.

Comp.	Left atrium			Right atrium			
	negative inotropy			negative inotropy			negative chronotropy
	Activity ^a (M ± SEM)	EC ₅₀ ^b (μM)	95% conf lim (×10 ⁻⁶)	Activity ^a (M ± SEM)	EC ₅₀ ^b (μM)	95% conf lim (×10 ⁻⁶)	Activity ^d (M ± SEM)
1	80 ± 1.7 ^e	0.43	0.31–0.55	87 ± 1.9 ^e	2.48	2.04–3.01	47 ± 0.9
2	93 ± 1.1 ^e	0.87	0.74–1.02	94 ± 2.7 ^e	1.08	0.80–1.19	37 ± 0.9
3	97 ± 1.9	0.22	0.13–0.35	97 ± 2.3	0.47	0.30–0.72	#
4	82 ± 2.5	1.91	1.64–2.21	92 ± 2.1	1.87	1.49–2.03	42 ± 2.6
5	65 ± 1.4 ^e	0.32	0.21–0.47	34 ± 1.2			8 ± 0.6 ^f
6	74 ± 2.2	1.49	1.06–1.88	79 ± 0.4	2.20	1.83–2.43	15 ± 0.3 ^g
7	79 ± 1.2	3.65	3.27–3.85	93 ± 1.1	2.18	1.77–2.43	37 ± 1.7 ^f
8	11 ± 0.3			4 ± 0.1 ^e			33 ± 2.1
9	75 ± 2.1	0.85	0.57–1.26	85 ± 1.6	2.87	2.43–3.03	26 ± 1.8 ^f
10	76 ± 1.4 ^e	1.91	0.93–3.10	85 ± 1.7 ^e	0.51	0.37–0.71	45 ± 1.4
Nif.	97 ± 2.0 ^e	0.26	0.19–0.36				85 ± 4.2 ^{h,i}

^a Decrease in developed tension on isolated guinea pig left atrium at 5×10^{-5} M, expressed as percent changes from the control (n = 5–6). The left atria were driven at 1 Hz. The 5×10^{-5} M concentration gave the maximum effect for most compounds.

^b Calculated from log concentration–response curves (Probit analysis by Litchfield and Wilcoxon [17] with n = 6–7). When the maximum effect was <50%, the EC₅₀ values were not calculated.

^c Decrease in developed tension on guinea pig spontaneously beating isolated right atrium at 5×10^{-5} M, expressed as percent changes from the control (n = 7–8). The 5×10^{-5} M concentration gave the maximum effect for most compounds.

^d Decrease in atrial rate on guinea pig spontaneously beating isolated right atrium at 10^{-5} M, expressed as percent changes from the control (n = 7–8). The 10^{-5} M concentration gave the maximum effect for most compounds. Pretreatment heart rate ranged from 165 to 190 beats/min.

^e At 10^{-5} M.

^f At 5×10^{-5} M & At 10^{-6} M.

^h At 10^{-7} M.

ⁱ EC₅₀ = 0.039 μM (c.l. 0.031–0.051). # Inactive up to the concentration indicated above.

2.2.3 Cytotoxicity

We investigated the effects of the best VGCC blockers (1e3, 10) on human neuronal SH-SY5Y cells viability by means of the color- imetric MTT assay. As depicted in Fig. 4, the loss of cell viability, after 48 h of exposure with compounds, was irrelevant and statistically non-significant.

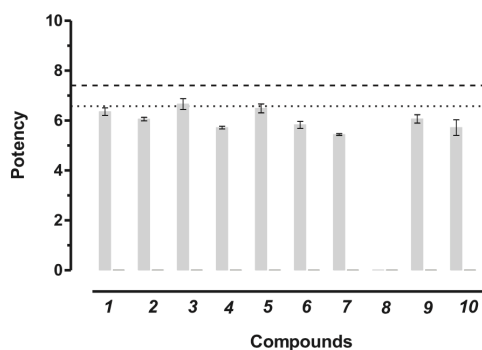


Fig. 2. Potency of compounds (pEC₅₀) on guinea pig cardiac parameters: negative inotropy (light grey) and negative chronotropy (dark grey). The dashed line shows the reference values of negative inotropic potency for NIF (pEC₅₀). The dotted line shows the reference values of negative chronotropic potency for NIF (pEC₅₀). When error bar are not shown, these are covered by the point itself.

2.2.4 GSK-3b activity

In order to test whether compounds 1-10 can also inhibit GSK-3b, we employed the LANCE Ultra TR-FRET assay, one of the most well established methods to determine kinase activity [19,20]. An initial screening was performed using a single concentration (10 mM) of each compound and the percentage of enzyme residual activity was calculated with respect to vehicle (DMSO). For comparison purpose, the reference standard compound SB216763 was also tested (IC₅₀ 1/4 11.4 ± 2.1 nM in our assay conditions).

Among the tested compounds, derivatives 3, 9 and 10 exhibited a weak but distinct inhibition of GSK-3b. In particular, it is note- worthy that this activity is related to the presence of a substituent in R1.

To ascertain whether the observed effect was dose-dependent, different concentrations were investigated and the results are displayed in Fig. 5. All the three tested compounds demonstrated an unambiguous dose-dependent effect in this assay, even with different biochemical potency.

Compound 10, bearing an N-heptylamide substituent, was the most potent of series (55% and 10% of GSK-3b residual activity at 3.12 mM and at 50 mM, respectively). In contrast, the elimination of the long alkyl chain reduced the inhibitor activity (48 and 51% of GSK-3b residual activity at 50 mM for 3 and 9, respectively).

Table 3
Activity of tested compounds on smooth muscle.

Compound	Aorta	Ileum		
	Activity ^a (M ± SEM)	Activity ^a (M ± SEM)	EC ₅₀ ^b (μM)	95% conf lim (×10 ⁻⁶)
1	21 ± 1.6	90 ± 1.7 ^c	3.33	2.77–3.02
2	9 ± 0.8	90 ± 1.4 ^e	1.18	0.89–1.32
3	7 ± 0.4	68 ± 2.4 ^c	0.49	0.31–0.66
4	8 ± 0.7	97 ± 1.6	14.66	12.19–17.38
5	6 ± 0.2	12 ± 0.		
6	#	90 ± 1.5 ^e	1.27	0.86–1.90
7	10 ± 0.7	67 ± 1.8 ^e	2.51	2.07–2.99
8	18 ± 0.7	85 ± 1.8	0.77	0.53–1.01
9	#	85 ± 2.4	12.06	11.09–12.73
10	6 ± 0.3	94 ± 3.8	3.67	2.74–4.91
Nif.	82 ± 1.3 ^{c,d}	70 ± 0.36 ^f	0.0015	0.0011–0.0022

^a Percent inhibition of calcium-induced contraction on K⁺-depolarized (80 mM) guinea pig aortic strips and longitudinal smooth muscle (at 5 × 10⁻⁵ M). The 5 × 10⁻⁵ M concentration gave the maximum effect for most compounds.

^b Calculated from log concentration-response curves (Probit analysis by Litchfield and Wilcoxon [17] with *n* = 6–7). When the maximum effect was <50%, the IC₅₀ values were not calculated.

^c At 10⁻⁶ M.

^d IC₅₀ = 0.009 μM (c.l. 0.003–0.020).

^e At 10⁻⁵ M / At 5 × 10⁻⁵ M # Inactive up to the concentration indicated above.

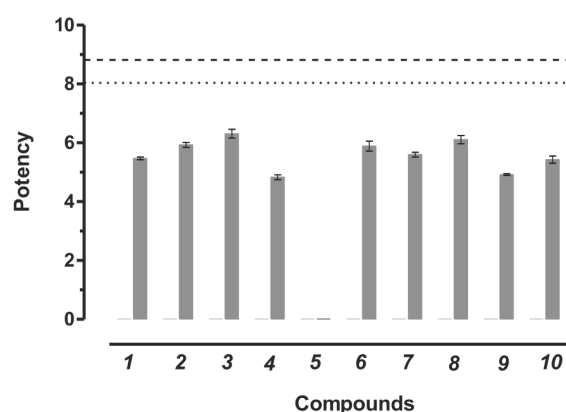


Fig. 3. Potency of compounds (pEC₅₀) on guinea pig smooth muscle parameters: vascular (aorta) (light grey) and non-vascular (ileum) (dark grey). The dashed line shows the reference potency values for NIF (pEC₅₀) on vascular tissues. The dotted line shows the reference potency values for NIF (pEC₅₀) on non-vascular tissues. When error bar are not shown, these are covered by the point itself.

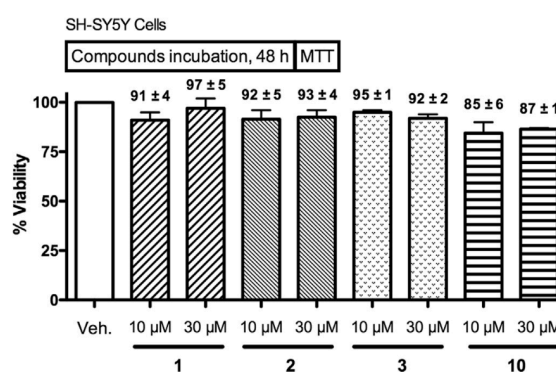


Fig. 4. Effect of compounds 1, 2, 3, and 10 on the viability of SH-SY5Y cells. SH-SY5Y cells were subjected to compounds for 48 h at 10 and 30 μM. Cell viability was measured by the method of the MTT reduction. Data are expressed as the mean ± SEM of cell viability compared with that of the basal group, i.e. cells only treated with vehicle (Veh. DMSO, white bar), of three independent experiments. Differences between basal and test groups were statistically not significant.

3. Discussion

It is well known that calcium imbalance in specific brain areas is involved in triggering neurodegeneration, and calcium channels modulators could be useful in diseases like AD [8]. Indeed, voltage- dependent currents, due to an increase in Ca^{2+} influx via LTCC, are enhanced in ageing hippocampal neurons [21], and LTCC antagonists could counteract this effect in aging-related diseases. Moreover, recent in vivo calcium imaging studies in a mouse model of AD have demonstrated aberrant increases in neuronal Ca^{2+} concentration close to Ab deposits [22]. A possible explanation could be that Ab peptides form Ca^{2+} - permeable pore in the plasma membrane, thereby rendering neurons vulnerable to excitotoxicity and apoptosis [7].

In a previous work, we have developed a series of LTCC blockers bearing a new maleimide-related polycyclic scaffold [9], which could also remind of the maleimide moiety found in recently re- ported GSK-3b inhibitors [11-14]. Given the long lasting experience of our research group in designing molecules for AD, we decided to exploit this new versatile structure to design a new series of compounds to be assessed for their potential therapeutic in AD.

First, the activity on the heart was evaluated to rule out any possible side effects. The compounds showed moderate negative inotropic properties and, unlike nifedipine, were all devoid of chronotropic activity, highlighting a remarkable selectivity. These results could reflect a different expression of Ca^{2+} channel subtypes in tissues used for functional assays. In particular, the negative inotropic effect is due to interaction with the Cav1.2 isoform, while the negative chronotropic effect seems to be related to interaction with the Cav1.3 isoform [23]. Furthermore, all compounds were devoid of vasorelaxant activity on aorta, being thus unable to affect the blood pressure.

Then, we evaluated the blocking activity of the new derivatives on SH-SY5Y neuroblastoma cells Ca^{2+} channels. This cell line ex- presses VGCC of neuronal type [24], and similar intracellular Ca^{2+} - buffering machinery to primary neural cultures, so it has been widely used to study the physiopathology of neurodegeneration and the effect of neuroprotective compounds directed to counteract Ca^{2+} overload. Compounds 1-3 and 10 inhibited the depolarization-stimulated calcium uptake into SH-SY5Y cells. In particular compound 10, with an IC_{50} of 9 mM, turned out to be the most potent VGCC blocker. It is well known that, like the heart, brain also expresses two sub-types of neuronal LTCCs, Cav1.2 (90%) and Cav1.3 (10%) isoforms, which regulate neuronal excitability and synaptic plasticity. Notably, in most cases, a single neuron ex- presses both of them [25,26]. Therefore, mitigation of Ca^{2+} entry excess elicited by 10 may restore the altered synaptic transmission and synaptic plasticity to normal parameters, ending the enhanced neuronal vulnerability.

Previous studies showed that 1 preferentially binds to inactivated LTCCs [9], therefore the same behavior can be speculated for 10, and this might also increase its therapeutic value by targeting only excitotoxic or pathologically active cells, thus sparing normal synapses [22,27].

Furthermore, 10 exhibited a slight but definitive inhibition of GSK-3b, the link between Ab and tau protein, the two major hallmarks of AD. GSK-3b inhibitors may improve deficient cognitive functions by reducing many inflammatory responses by both astrocytes and microglia in the CNS. Our organism is not prepared to restore the overexpression of this enzyme in different pathological conditions such as AD, thus a smooth inhibition of GSK-3b, able to decrease levels of activity to physiological ones, would be enough to produce an important therapeutic effect [28]. In this way, a moderate inhibition restores GSK-3b activity to normal levels in a disease-affected tissue, with negligible effect on healthy tissues. Notably, compound 10 contains an amide bond, widespread in drug candidates, that, due to its intrinsic stability, represents a privileged motif in medicinal

chemistry.

In summary, a series of polycyclic maleimide-based derivatives were designed and synthesized as dual calcium channels and GSK-3 β modulators for AD treatment. The new compounds showed interesting properties on the selected targets, highlighting the potential of this easily affordable polycyclic scaffold as a new privileged structure in medicinal chemistry. From a multitarget point of view, 10 represents a promising non-toxic lead compound, bypassing the cardiovascular side effects resulting from peripheral L-type channel blockade and embracing in a new atypical scaffold calcium modulating brain-addressed properties and GSK-3 β properly adjusted inhibitory activity.

Table 4
Blockade of the Ca²⁺ entry elicited by K⁺ 70 mM-evoked depolarization in SH-SY5Y cells by derivatives 1–10, measured by the Ca²⁺-sensitive probe Fluo-4^a.

Compound	% Blockade ^b	IC ₅₀ μ M
Nimodipine	25 \pm 5	14 \pm 5
1	39 \pm 14	15 \pm 4
2	37 \pm 11	11 \pm 1
3	38 \pm 12	15 \pm 5
4	11 \pm 14	
5	0 \pm 11	
6	6 \pm 3	
7	8 \pm 13	
8	20 \pm 15	
9	4 \pm 9	
10	56 \pm 9	9 \pm 3

^a Data are mean of at least three independent experiments \pm SEM in triplicates, comparing with the K⁺-induced Ca²⁺ increase in the absence of compounds.

^b Compounds evaluated at 10 μ M.

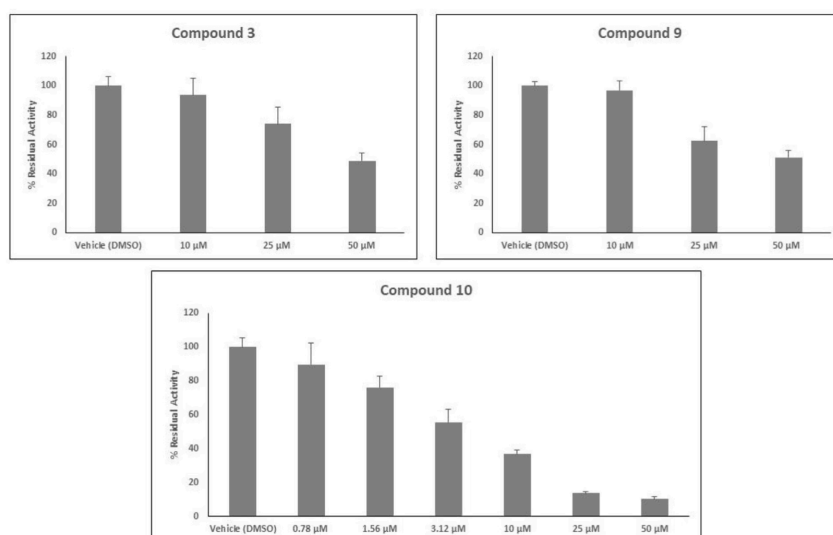


Fig. 5. Effect of compounds 3, 9 and 10 on GSK-3 β enzymatic activity. The activity of the compounds on GSK-3 β was determined using a TR-FRET assay. Each compound inhibited the enzyme in a dose-dependent manner. Values obtained for each compound are the means \pm SD determined for three separate experiments.

4. Experimental

4.1 Chemistry

4.1.1 General methods

Melting points were measured in glass capillary tubes on a Büchi SMP-20 apparatus and are uncorrected. NMR spectra were recorded in CDCl₃, unless otherwise indicated, on a Varian Gemini spectrometer at 400 MHz (1H) and 100 MHz (13C). Chemical shifts are reported in parts per million (ppm) relative to tetramethylsilane (TMS), and spin multiplicities are given as s (singlet), d (doublet), t (triplet), m (multiplet) or br (broad). Direct infusion ES-MS spectra were recorded on a Waters Micromass ZQ 4000 apparatus. High resolution mass spectra (HRMS) were recorded on a Waters Xevo Q-ToF. Chromatographic separations were performed by flash chromatography on silica gel

columns (Kieselgel 40, 0.040e0.063mm; Merck). Organic solutions were dried over anhydrous sodium sulfate. Elemental analysis was used to determine purity of the described compounds. All chemicals were purchased from Aldrich Chemistry, Milan (Italy), or from Alfa Aesar, Milan (Italy), and were of the highest purity. Compounds were named relying on the naming algorithm developed by CambridgeSoft Corporation and used in ChemDraw Professional 15.0.

4.1.2. General procedure for the synthesis of compounds 1e10 via Diels-Alder cycloaddition

A solution of maleimide (1.0 mmol) and the selected anthracene derivative (1.0 mmol) in toluene was refluxed for 3 h and allowed to stand overnight. The reaction mixture was then heated under reflux for another 90min. After cooling, the precipitate was collected by filtration and purified by recrystallization from ethyl acetate, unless otherwise indicated.

4.1.2.1. 2-chloro-9,10-dihydro-9,10- [3,4]epipyrroloanthracene-12,14- dione (1). Using the previous procedure and starting from 2- chloroanthracene, 1 was obtained [9].

4.1.2.2. 1-chloro-9,10-dihydro-9,10- [3,4]epipyrroloanthracene- 12,14-dione (2). Using the previous procedure and starting from 1- chloroanthracene, 2 was obtained [9].

4.1.2.3. 9,10-dichloro-9,10-dihydro-9,10- [3,4]epipyrroloanthracene- 12,14-dione (3). Using the previous procedure and starting from 9,10-dichloroanthracene 12, 3 was obtained. Yield 36%, mp > 250 °C. ¹H NMR d: 3.50 (s, 2H), 7.26e7.40 (m, 4H Ar), 7.74e7.76 (m, 2H Ar), 7.85e7.87 (m, 2H Ar), 9.38 (br, 1H, NH). ¹³C NMR d: 55.56 (2CH), 62.92 (2C), 123.09, 123.65, 128.56, 128.96, 136.79, 139.93, 171.50 (2CO). ESI-MS (m/z): 366 (M + Na). HRMS ESI + [M + 23]: calcd for C₁₈H₁₁Cl₂NO₂Na, 366.0064. Found: 366.0066.

4.1.2.4. 1-amino-9,10-dihydro-9,10- [3,4]epipyrroloanthracene- 12,14-dione (4). Using the previous procedure and starting from anthracen-1-amine (13), 4 was obtained. The product was then converted in the hydrochloride salt affording 4.HCl. Yield 6%, mp > 250 °C (MeOH/ethyl ether). ¹H NMR d: 3.24-3.28 (m, 2H), 4.67 (d, J 1/4 9.6 Hz, 2H), 6.59-6.76 (m, 1H Ar), 6.78-6.81 (m, 1H Ar), 7.05-7.18 (m, 1H Ar), 7.19e7.21 (m, 1H Ar), 7.25e7.29 (m, 2H Ar), 7.32e7.34 (m, 2H Ar), 7.53 (br, 2H, NH₂). ¹³C NMR d: 44.83 (CH), 47.12 (CH), 47.65 (CH), 47.77 (CH), 120.98, 125.15, 126.01 (2C), 126.85 (2C), 126.98, 127.13, 127.66, 138.83, 139.42, 144.97 (CNH₂), 177.98 (CO), 178.32 (CO). ESI-MS (m/z): 291 (M + H⁺). HRMS ESI + [M + 1]: calcd for C₁₈H₁₅N₂O₂, 291.1133. Found: 291.1131.

4.1.2.5. N-(12,14-dioxo-9,10-dihydro-9,10- [3,4]epipyrroloanthracen- 1-yl)acetamide (5). Using the previous procedure and starting from 14, 5 was obtained. Yield 25%, mp 182-183 °C. ¹H NMR d: 2.16 (s, 3H), 3.25e3.27 (m, 2H), 4.81 (d, J 1/4 4.4 Hz, 2H), 7.21-7.58 (m, 7H Ar). ¹³C NMR d: 23.98 (CH₃), 40.61 (CH), 46.47 (CH), 48.65 (CH), 48.91 (CH), 122.21, 122.39, 122.49, 124.79, 125.56, 127.09, 127.25, 132.58, 135.82, 141.27, 142.48, 143.15, 168.92 (COCH₃), 177.80 (CO), 178.13 (CO). ESI-MS (m/z): 355 (M + Na). HRMS ESI + [M + 23]: calcd for C₂₀H₁₆N₂O₃Na, 355.1059. Found: 355.1058.

4.1.2.6. 2-amino-9,10-dihydro-9,10- [3,4]epipyrroloanthracene- 12,14-dione (6). Using the previous procedure and starting from anthracen-2-amine (15), 6 was obtained. Yield 93%. mp > 250 °C. ¹H NMR d: 3.22e3.26 (m, 2H), 3.64 (br, 2H, NH₂), 4.65 (d, J 1/4 9.6 Hz, 2H), 6.44e6.75 (m, 1H Ar.), 6.66-6.75 (m, 1H Ar), 7.05-7.24 (m, 3H Ar), 7.32-7.34 (m, 2H Ar). ¹³C NMR d: 44.95 (CH), 46.18 (CH), 47.83 (CH), 48.61 (CH), 106.83, 121.44, 124.61, 125.66, 126.31, 127.09, 127.48, 128.82, 138.29, 139.08, 140.36, 144.62 (CNH₂), 177.38 (CO), 178.22 (CO). ESI-MS (m/z): 291 (M + H⁺), 313 (M + Na). HRMS ESI + [M + 23]: calcd for C₁₈H₁₄N₂O₂Na, 313.0953. Found: 313.0955.

4.1.2.7. 2-acetyl-9,10-dihydro-9,10- [3,4]epipyrroloanthracene-12,14- dione (8). Using the previous procedure and starting from 1- (anthracen-2-yl)ethan-1-one (16), 8 was obtained. Yield 35%, mp 244-245 °C. ¹H NMR d: 2.58 (d, J 1/4 10.4 Hz, 3H), 3.26-3.32 (m, 2H), 4.85 (t, J 1/4 3.2 Hz, 2H), 7.18-7.24 (m, 2H Ar), 7.32-7.49 (m, 3H Ar.), 7.79-7.97 (m, 2H Ar). ¹³C NMR d: 26.63 (CH₃), 45.30 (CH), 45.32 (CH), 47.59 (CH), 47.85 (CH), 124.38, 124.75, 125.25, 125.26, 125.31, 127.41, 127.54, 136.01, 139.24, 140.87, 141.94, 144.00, 176.20 (CO), 176.25 (CO), 197.57 (COCH₃). ESI-MS (m/z): 340 (M + Na). HRMS ESI + [M + 23]: calcd for C₂₀H₁₅NO₃Na, 340.0950. Found: 340.0949.

4.1.2.8. 9-((benzylimino)methyl)-9,10-dihydro-9,10- [3,4]epi- pyrroloanthracene-12,14-dione (9). Using the previous procedure and starting from 17, 9 was obtained. Yield 87%, mp 243-245 °C. ¹H NMR d: 3.35 (d, J 1/4 3.1 Hz, 1H), 3.81 (d, J 1/4 3.1 Hz, 1H), 4.82 (s, 1H), 5.11-5.22 (m, 2H), 7.08-7.61 (m, CH + 13H Ar). ¹³C NMR d: 45.91 (C), 48.96 (CH), 50.12 (CH), 52.43 (CH), 65.90 (CH₂), 123.55, 123.89, 124.09, 125.48, 126.50, 127.00, 127.13, 127.17 (2C), 127.23, 128.31, 128.68 (2C), 138.37, 138.79, 138.96, 141.41, 141.86, 162.17 (C1/4N), 175.48 (CO), 176.14 (CO). ESI-MS (m/z): 393 (M + H⁺), 415 (M + Na). HRMS ESI + [M + 23]: calcd for C₂₆H₂₀N₂O₂Na, 415.1422. Found: 415.1424.

4.1.2.9. N-heptyl-12,14-dioxo-9,10- [3,4]epipyrroloanthracene- 9(10H)-carboxamide (10). Using the previous procedure and starting from 18, 10 was obtained. Yield 45%, mp 180-182 °C. ¹H NMR d: 0.91 (t, J 1/4 6.8 Hz, 3H), 1.26-1.35 (m, 4H), 1.42-1.51 (m, 4H), 1.72-1.81 (m, 2H), 3.28 (dd, J 1/4 8.8 and 3.2 Hz, 1H), 3.55-3.73 (m, 3H), 4.77 (d, J 1/4 2.8 Hz, 1H), 7.21-7.24 (m, 3H Ar), 7.32-7.40 (m, 4H Ar), 7.49-7.51 (m, 1H Ar). ¹³C NMR d: 14.22 (CH₃), 22.75 (CH₂), 27.24 (CH₂), 29.14 (CH₂), 29.70 (CH₂), 31.92 (CH₂), 40.24 (CH₂N), 45.83 (CH), 48.87 (CH), 50.45 (C), 59.09 (CH), 123.77, 124.71, 124.89, 125.62, 127.07, 127.50, 127.57, 127.72, 137.64, 137.92, 140.82, 140.90, 168.36 (CO), 175.50 (CO), 176.31 (CO). ESI-MS (m/z): 439 (M + Na). HRMS ESI + [M + 23]: calcd for C₂₆H₂₈N₂O₃Na, 439.1998. Found: 439.2000.

4.1.3. General procedure for the synthesis of amide compounds 7, 14

A stirred mixture of the selected amine (1 eq.), acetylchloride (1.1 eq.) and K₂CO₃ in acetone (40 mL) was refluxed for 3 h. The hot reaction mixture was filtered and evaporated to dryness. The crude residue was purified via flash column chromatography (toluene/ acetone 4:1).

4.1.3.1. N-(12,14-dioxo-9,10-dihydro-9,10- [3,4]epipyrroloanthracen- 2-yl)acetamide (7). Using the previous procedure and starting from 6, 7 was obtained (23% yield), mp 174-175 °C. ¹H NMR d: 2.16 (d, J 1/4 12.8 Hz, 3H), 3.25-3.27 (m, 2H), 4.76 (d, J 1/4 4.4 Hz, 2H), 7.15-7.45 (m, 7H Ar). ¹³C NMR d: 23.99 (CH₃), 40.65 (CH), 46.58 (CH), 48.75 (CH), 48.96 (CH), 122.25, 122.41, 122.52, 124.67, 125.77, 127.19, 127.83, 132.59, 136.02, 141.29, 142.53, 143.65, 168.96 (COCH₃), 177.85 (CO), 178.38 (CO). ESI-MS (m/z): 333 (M + H⁺), 355 (M + Na). HRMS ESI + [M + 23]: calcd for C₂₀H₁₆N₂O₃Na, 355.1059. Found: 355.1057.

4.1.3.2. N-(anthracen-1-yl)acetamide (14). Using the previous procedure and starting from anthracen-1-amine (13), 14 was obtained. Yield 56%, mp 202-204 ° C. ¹H NMR d: 2.42 (s, 3H), 3.98 (br, 1H, NH), 7.2-8.6 (m, 9H Ar). ¹³C NMR d: 24.12, 108.83, 118.84, 119.25, 121.22, 125.63, 125.77, 125.96, 126.88, 128.18, 128.75, 130.47, 131.49, 132.38, 142.24, 168.91.

4.1.4. 1-(anthracen-9-yl)eN-benzylmethanimine (17)

A mixture of anthracene-9-carbaldehyde (0.5 g, 2.43 mmol) and benzylamine (0.29 g, 2.67 mmol) in toluene (40 mL) was refluxed for 24 h with Dean-Stark apparatus. The mixture was washed with water (3 25 mL), and the organic layer was evaporated under reduced pressure. The residue was

purified by flash chromatography affording 13 (0.18 g, 26% yield), mp 70-72 °C (ligroin). ¹H NMR d: 5.21 (s, 2H), 7.23e8.61 (m, 12H Ar), 8.79 (s, 1H, CH 1/4), 9.01 (d, 1H Ar), 9.59 (s, 1H Ar). ¹³C NMR d: 64.51, 123.92, 125.31, 125.43, 125.77, 127.94, 128.16, 128.47, 128.35, 128.42, 130.99, 131.78, 135.38, 138.92, 160.86.

4.1.5. N-heptylanthracene-9-carboxamide (18) Anthracene-9-carboxylic acid (1 g, 4.4 mmol) was treated with SOCl₂ (0.66 mL, 8.8 mmol) and the mixture was heated on a steam bath for 4h, the excess of SOCl₂ was removed under reduced pressure and the resulting acyl chloride was added to a solution of n-heptylamine (0.33 mL, 2.2 mmol) and TEA (0.61 mL, 4.4 mmol) in CH₂Cl₂ (3 mL). The mixture was stirred 3 h at rt and poured in ice/ water. The mixture was extracted with ethyl acetate, washed with water, dried over Na₂SO₄ and evaporated to dryness, to obtain the desired compound, which was used for the following step without further purification.

4.2. Biology

4.2.1. Functional studies

The pharmacological profile of all compounds was derived on guinea-pig isolated left and right atria to evaluate their inotropic and chronotropic effects, respectively, and on K⁺-depolarized (80mM) guinea-pig vascular (aortic strips) and non vascular (ileum) smooth muscle to assess calcium antagonist activity. All procedures followed the guidelines of animal care and approved by the Ethics Committee of the University of Bologna (Bologna, Italy) (ID: 737/2017). The methods were previously described [29]. Briefly, compounds were checked at increasing doses (0.1, 0.5, 1, 5, 10, 50, 100 mMol/L) to evaluate the percent decrease of developed tension on isolated left atrium driven at 1 Hz (negative inotropic activity), the percent decrease in atrial rate on spontaneously beating right atrium (negative chronotropic activity). For compounds devoid of negative chronotropic activity, the inotropy was also checked in spontaneously beating right atria. The percent inhibition of calcium-induced contraction was evaluated on K⁺- depolarized smooth muscle strips.

Data were analyzed using Student's t-test and presented as mean ± S.E.M [17]. Since the drugs were added in cumulative manner, the differences between the control and the experimental values at each concentration were tested for a P value < 0.05. The potency of drugs defined as EC₅₀ and IC₅₀ was evaluated from log concentration-response curves (Probit analysis using Litchfield and Wilcoxon [17] or GraphPad Prism® software [30,31] in the appropriate pharmacological preparations).

4.2.2. SH-SY5Y neuroblastoma cells culture

The SH-SY5Y neuroblastoma cell line was acquired from ATCC (Manassas, USA; cat#CRL-2266). Cells were kept at 37 ° C under humidity and an atmosphere enriched with 5% CO₂. Cell batches of low number of passages lacked mycoplasma, according to the Mycoplasma detection kit QuickTest (Houston, USA) assay. Cells maintenance and culture were performed according to what have been described [18]. All the experiments were conducted in sterile conditions.

4.2.3. Fluorescence-based Ca²⁺ increases measurements

Following a protocol recently described [18], SH-SY5Y neuroblastoma cells, seeded in clear-bottom, black 96-well plates, and with 100% of confluence (36-72h after seeding), were charged with the Ca²⁺-sensitive Fluo-4 dye (Life Technologies, Alcobendas, Spain) in its pro-drug form (acetoxymethyl ester) at 10mM in Krebs-HEPES buffer (composition in mM: 145 NaCl, 5.6 KCl, 1.2 MgCl₂, 2 CaCl₂, 11 glucose, and 10 HEPES; pH 7.4) for 45 min, along with pluronic acid 0.2%, used to facilitate its entry through the plasma membrane. Then, cells were gently washed out with

Krebs- HEPES and incubated with compounds at the desired concentration or vehicle (DMSO) for 10min. Afterwards, SH-SY5Y cells were exposed to K⁺ 70 mM by injecting a solution with high KCl concentration, inducing cell depolarization and subsequent Ca²⁺ increase, which was monitored by reading the Fluo-4-derived fluorescence in a multi-well fluorescence reader (FluoStar Optima, BMG Labtech, Ortenberg, Germany). To calculate the Ca²⁺ increase in presence of compounds compared with the control situation, fluorescence in each well was obtained according to the following formula: $D[Ca^{2+}]_c = \frac{1}{4} \frac{(F_x - F_0)}{(F_{max} - F_{min})}$, whereby F_x is the maximal fluorescence reached, F_0 is the average fluorescence before injecting the solution of high K⁺, F_{max} is the fluorescence obtained after treating cells with 5% Triton X (100 mL), used to lysate cells and recover the maximal fluorescence of the well, and F_{min} is the fluorescence obtained when 100 mL of MnCl₂ 1M were applied to the cell lysate, which fully quenched the fluorescent dye, thus obtaining the minimum fluorescence. After monitoring the Ca²⁺ oscillations for 2 min, F_{max} then F_{min} were obtained by successive addition of the Triton, then the MnCl₂ solutions. Compounds were evaluated in a blind fashion.

4.2.4. Toxicity assays

SH-SY5Y cells were maintained similarly to what was previously described [32]. Cells were seeded in 48-well plates at a seeding density of 70 000 cells/well. Before cells confluence, compounds dissolved in MEM/F12 media supplemented with 10% fetal bovine serum (FBS) were preincubated for 24 h. Then, media was replaced by fresh new media with 1% FBS and compounds and the culture maintained for 24h more. Then, the colorimetric dye 3-[4,5- dimethylthiazole-2-il]-2,5-diphenyltetrazolium bromide (MTT) was applied to cells at the concentration of 1.2 mM and incubated for 2 h in dark. Media were removed and the precipitated, purple- colored formazan, generated by the reduction of MTT, was dissolved with 0.3 mL of DMSO. Solutions were transferred to a 96-well plate to measure the absorbance of each well at 540 nm in a multi-well plate reader, whereby the more purple absorbance, the more cell viability. Cells non-treated with compounds defined the maximal cell viability, normalized to 100%, and SH-SY5Y cells exposed to compounds showed a cell viability of the expressed percentage compared with the basal group.

4.2.5. GSK-3b inhibition

The assays were performed in white Optiplat-384 at room temperature (22 °C) in a final volume of 25 mL, using the following Kinase Buffer: 50 mM HEPES pH 7.5, 1 mM EGTA, 10 mM MgCl₂, 2 mM DTT and 0.01% Tween-20. The compounds were dissolved in DMSO and then diluted in kinase buffer, keeping constant the concentration of DMSO (3%) in each well. In each assay, the compound SB216763 was used as positive control (IC₅₀ 11.4 ± 2.1 nM), while DMSO was used as reference. GSK-3b (0.5 nM, final concentration) was first incubated with the three compounds for 30 min, then a mixture of ATP (10 mM, final concentration) and ULight-GS (Ser641/pSer657) Peptide (50 nM, final concentration) was added. The reaction was incubated for 1 h, afterwards the kinase reaction was stopped by adding 24 mM EDTA and 2 nM (final concentration) of Eu-anti-phospho-GS (Ser641) antibody, both diluted in Detection Buffer 1. After an incubation of 1 h, the TR-FRET signal was read with the EnSight Multimode Plate Reader (excitation at 320 nm and emissions at 615 and 665 nm). Values obtained for each compound are the means ± SD determined for three separate experiments. The tested compounds are soluble in the assay conditions as determined at the maximum concentration tested (nephelometry determination).

Appendix A. Supplementary data

References

- [1] M. Prince, A. Wimo, M. Guerchet, G.-C. Ali, Y.-T. Wu, M. Prina, World Alzheimer Disease Report, Alzheimer's Disease International, London, UK, 2015, pp. 25-46.
- [2] J.R. Morphy, Chapter 10 the challenges of multi-target lead optimization, in: J.R. Morphy, C.J. Harris (Eds.), Designing Multi-target Drugs, The Royal Society of Chemistry, London, 2012, pp. 141-154.
- [3] N.J. Ortner, J. Striessnig, L-type calcium channels as drug targets in CNS disorders, *Channels* 10 (1) (2016) 7-13.
- [4] G.W. Zamponi, Targeting voltage-gated calcium channels in neurological and psychiatric diseases, *Nat. Rev. j Drug Discov.* 15 (2016) 19-34.
- [5] D.J. Triggle, L-type calcium channels, *Curr. Pharmaceut. Des.* 12 (4) (2006) 443-457.
- [6] R. Resende, C. Pereira, P. Agostinho, A.P. Vieira, J.O. Malva, C.R. Oliveira, Susceptibility of hippocampal neurons to Ab peptide toxicity is associated with perturbation of Ca²⁺ homeostasis, *Brain Res.* 1143 (2007) 11-21.
- [7] G. Zundorf, G. Reiser, Calcium dysregulation and homeostasis of neural calcium in the molecular mechanisms of neurodegenerative diseases provide multiple targets for neuroprotection, *Antioxidants Redox Signal.* 14 (2011) 1275-1288.
- [8] V. Nimmrich, A. Eckert, Calcium channel blockers and dementia, *Br. J. Pharmacol.* 169 (2013) 1203-1210.
- [9] S. Bova, S. Saponara, A. Rampa, S. Gobbi, L. Cima, F. Fusi, G. Sgaragli, M. Cavalli, C. de los Rios, J. Striessnig, A. Bisi, Anthracene based compounds as new L-type Ca²⁺ channel blockers: design, synthesis, and full biological profile, *J. Med. Chem.* 52 (5) (2009) 1259-1262.
- [10] A. Bisi, S. Gobbi, L. Merolle, G. Farruggia, F. Belluti, A. Rampa, J. Molnar, E. Malucelli, C. Cappadone, Design, synthesis and biological profile of new inhibitors of multidrug resistance associated proteins carrying a polycyclic scaffold, *Eur. J. Med. Chem.* 92 (2015) 471-480.
- [11] D.G. Smith, M. Buffet, A.E. Fenwick, D. Haigh, R.J. Ife, M. Saunders, B.P. Slingsby, R. Stacey, R.W. Ward, 3-Anilino-4-arylmaleimides: potent and selective inhibitors of glycogen synthase kinase-3 (GSK-3), *Bioorg. Med. Chem. Lett* 11 (2001) 635-639.
- [12] Q. Ye, Y. Shen, Y. Zhou, D. Lv, J. Gao, J. Li, Y. Hu, Design, synthesis and evaluation of 7-azaindazolyl-indolyl-maleimides as glycogen synthase kinase-3b (GSK-3b) inhibitors, *Eur. J. Med. Chem.* 68 (2013) 361-371.
- [13] Q. Ye, W. Mao, Y. Zhou, L. Xu, Q. Li, Y. Gao, J. Wang, C. Li, Y. Xu, Y. Xu, H. Liao, L. Zhang, J. Gao, J. Li, T. Pang, Synthesis and biological evaluation of 3-([1,2,4] triazolo[4,3-a]pyridin-3-yl)-4-(indol-3-yl)-maleimides as potent, selective GSK-3b inhibitors and neuroprotective agents, *Bioorg. Med. Chem.* 23 (2015) 1179-1188.
- [14] Q. Ye, M. Li, Y. Zhou, T. Pang, L. Xu, J. Cao, L. Han, Y. Li, W. Wang, J. Gao, J. Li, Synthesis and biological evaluation of 3-Benzisoxazolyl-4-indolylmaleimides as potent, selective inhibitors of glycogen synthase kinase-3b, *Molecules* 18 (2013) 5498-5516.

- [15] M. Llorens-Martín, J. Jurado, F. Hernandez, J. Avila, GSK-3b, a pivotal kinase in Alzheimer disease, *Front. Mol. Neurosci.* 7 (46) (2017) 1-11.
- [16] I. Khan, M.A. Tantray, M. Sarwar Alam, H. Hamid, Natural and synthetic bioactive inhibitors of glycogen synthase kinase, *Eur. J. Med. Chem.* 125 (2017) 464-477.
- [17] R.J. Tallarida, R.B. Murray, *Manual of Pharmacologic Calculations with Computer Programs*, second ed., Springer-Verlag, New York, 1987.
- [18] R. Lajarín-Cuesta, C. Nanclares, J.-A. Arranz-Tagarro, L. Gonzalez-Lafuente, R.L. Arribas, M. Araujo de Brito, L. Gandía, C. de los Ríos, Gramine derivatives targeting Ca²⁺ channels and ser/thr phosphatases: a new dual strategy for the treatment of neurodegenerative diseases, *J. Med. Chem.* 59 (2016) 6265-6280.
- [19] D.J. Moshinsky, L. Ruslim, R.A. Blake, F. Tang, A widely applicable, high- throughput TR-FRET assay for the measurement of kinase autophosphorylation: VEGFR-2 as a prototype, *J. Biomol. Screen* 8 (2003) 447-452.
- [20] D. Patnaik, X. Jun, M.A. Glicksman, G.D. Cuny, R.L. Stein, J.M.G. Higgins, Identification of small molecule inhibitors of the mitotic kinase haspin by high-throughput screening using a homogeneous time-resolved fluorescence resonance energy transfer assay, *J. Biomol. Screen* 13 (2008) 1025-1034.
- [21] M.J. Berridge, Calcium regulation of neural rhythms, memory and Alzheimer's disease, *J. Physiol.* 592 (2014) 281-293.
- [22] J.-A. Arranz-Tagarro, C. de los Rios, A.G. Garcia, J.-F. Padin, Recent patents on calcium channel blockers: emphasis on CNS diseases, *Expert Opin. Ther. Pat.* 24 (9) (2014) 959-977.
- [23] K.V. Kuchibhotla, S.T. Goldman, C.R. Lattarulo, H.Y. Wu, B.T. Hyman, B.J. Bacskai, A β plaques lead to aberrant regulation of calcium homeostasis in vivo resulting in structural and functional disruption of neuronal networks, *Neuron* 59 (2008) 214-225.
- [24] S.R. Sousa, I. Vetter, L. Ragnarsson, R.J. Lewis, Expression and Pharmacology of endogenous Cav channels in SH-SY5Y human neuroblastoma cells, *PloS One* 8 (3) (2013) e59293.
- [25] J. Striessnig, A. Pinggera, G. Kaur, G. Bock, P. Tuluc, L-type Ca²⁺ channels in heart and brain, *WIREs Membr. Transp. Signal.* 3 (2014) 15-38.
- [26] G.W. Zamponi, J. Striessnig, A. Koschak, A.C. Dolphin, The physiology, pathology, and pharmacology of voltage-gated calcium channels and their future therapeutic potential, *Pharmacol. Rev.* 67 (2015) 821-870.
- [27] S. Navakkodea, L. Chao, T.W. Soong, Altered function of neuronal L-type calcium channels in ageing and neuroinflammation: implications in age-related synaptic dysfunction and cognitive decline, *Ageing Res. Rev.* 42 (2018) 86-99.
- [28] A. Martinez, D.I. Perez, C. Gil, Lessons learnt from glycogen synthase kinase 3 inhibitors development for Alzheimer's disease, *Curr. Top. Med. Chem.* 13 (2013) 1808-1819.

- [29] M. Micucci, A. Angeletti, M. Cont, I. Corazza, R. Aldini, E. Donadio, A. Chiarini, R. Budriesi, Hibiscus Sabdariffa L. flowers and Olea Europea L. leaves extract-based formulation for hypertension care: in vitro efficacy and toxicological profile, J. Med. Food 19 (2016) 504-512.
- [30] H. Motulsky, A. Christopoulos, Fitting models to biological data using linear and non linear regression. www.graphpad.com, 2003.
- [31] H.J.Motulsky, Prism 5 Statistics Guide, Graph Pad Software Inc., SanDiego,CA, 2007. www.graphpad.com.
- [32] L. Gonzalez-Lafuente, J. Egea, R. Leon, F.J. Martinez-Sanz, L. Monjas, C. Perez, C. Merino, A.M. Garcia-De Diego, M.I. Rodriguez-Franco, A.G. Garcia, M. Villarroya, M.G. Lopez, C. de Los Rios, Benzothiazepine CGP37157 and its isosteric 2'-methyl analogue provide neuroprotection and block cell calcium entry, ACS Chem. Neurosci. 3 (2012) 519-529.